Applied Environmental Research
- RESEARCH FOR SUSTAINABLE PLANET -

Research Article

Removal of Chromium from Aqueous System Using Nanocellulose Prepared from Defoliated Terminalia Catappa Leaves

Lopamudra Digal, Jayashree Mohanty*

C.V. Raman Global University, India

*Correspondence Email: jayashreemohanty7@gmail.com

Abstract

Nanocellulose is considered as a sustainable and renewable nanomaterial due to its abundant availability, biodegradability and biocompatibility characteristics. The study demonstrates the synthesis of nanocellulose from defoliated leaves of the Tropical Almond (Terminalia catappa) plant, abundantly available residual plant biomass and its subsequent use in eliminating Cr(VI) from the water system. The study demonstrates the preparation of nanocellulose by chemical means, employing NaOH and H_2SO_4 as chemical agents. Characterization techniques like FTIR, SEM, and XRD were used to study the chemical composition and morphology of the resulting nanocellulose. The characterization studies confirm the formation of nanocellulose from the plant biomass. The Cr(VI) adsorption study of the produced nanocellulose is carried out through fitting different adsorption isotherm models and kinetic models. According to the study, Cr(VI) adsorption gradually increases as time period of treatment increases. A maximum adsorption of 98.4% is attained for time period of treatment of 75 min. Overall, the study proposes mixed types of adsorption (chemisorption and physisorption) of Cr(VI) on nanocellulose. This comprehensive research contributes in developing affordable, sustainable nanobiomass from plentiful bio-waste for use in the removal of heavy metals from water streams.

ARTICLE HISTORY

Received: 4 Jul. 2023
Accepted: 2 Apr. 2024
Published: 25 Jun. 2024

KEYWORDS

Terminalia catappa;
Nanocellulose;
Defoliated leaves;
Chromium removal;
Aqueous system

Introduction

Over the past few years, nanocellulose has received lots of attention for its unique properties, such as plentiful availability in nature, biocompatibility, cost-effectiveness and sustainable characteristics [1–3]. Due to its various attractive characteristics including light-weight, high surface area, high modulus, tensile strength, chemical inertness and low coefficient of thermal expansion combined with its propensity for easy surface modification, make it a promising biomaterial with a wide range of potential uses, including as reinforcing agents in polymers to create biodegradable bio-nanocomposites, as well as potential uses in the paper, construction, automotive, electronics and medical industries [4–8].

The various characteristics ofthe nanocellulose depend upon the synthesis as well as the natureof the biomass source from which it is produced. In the current context, the topic of producing nanocellulose from diverse feedstocks with a range of features and possible applications is seen as a promising area of research [4]. Conventionally, the synthesis of nanocellulose from lignocellulosic biomass involves two main stages: (i) pre-treatment of biomass to extract cellulose and (ii) conversion of extracted cellulose into nanocellulose through hydrolysis. Usually, the hydrolysis is carried out using dilute sulfuric acid as the hydrolyzing agent [9] and before hydrolysis pre-treatment is carried out for removal of lignin and hemicelluloses with simultaneous isolation of cellulose [10].

https://doi.org/10.35762/AER.2024022

In this regard, nanocellulose has been prepared from various cellulosic/lignocellulosic biomass such as fruit fiber of C. Procera [9], Pennisetum hydridum [10] fertilized by municipal sewage sludge [11], Kenaf paste fibers [12], Ramie fibers [13], corn cob [14], bamboo [15], rice husk [16], hardwoods [17], pine-apple leaves [18], palm residues [19] etc. Defoliated plant leaves constitute one of the major readily available residual plant biomasses in every region of the world. The extraction of nanocellulose, from such residual plant biomass will not only provide the sustainable preparation of the said nano biomass but also deliver a method of value-added utilization of this biomass waste [20].

In general practice, defoliated plant leaves are mostly discarded by landfilling or burning, which results in air pollution [21]. Trees like the tropical almond (Terminalia catappa), found throughout the tropics, undergo a brief period of deciduousness either during the dry season or, in certain environments and may experience leaf shedding twice a year [22]. Due to the abundant availability along with adequate cellulose content, such defoliated plant leaves can be considered as a suitable feedstock for the sustainable extraction of 56 nanocellulose for its further potential applications [23].

Heavy metal like chromium has widespread applications in various industrial processes such as electroplating, printing, dyeing, tanning and metallurgy. Direct or indirect disposal of effluents from these industries results in environmental pollution. Chromium (Cr) most commonly occurs in trivalent and hexavalent states. Out of the two oxidation states of Cr, the hexavalent state is non-essential and toxic to animals and may cause dermatitis, lung cancer, kidney and gastric damage and irritation to the respiratory tract and eyes. Chronic build-up of harmful hexavalent chromium (Cr(VI)) in food chains leads to bio-magnification which increases the risk to humans [24].

There are many conventional processes currently in use for the remediation of Cr(VI) from industrial effluents out of which adsorption is considered to be an effective method due to the low initial cost, flexibility in design, and ease of operation. Additionally, adsorption does not result in the formation of sludge or other secondary wastes. Biosorption is a subdivision of adsorption, in which Cr(VI) is adsorbed onto biomaterials [24].

Nanomaterials have proven to be very stable and have larger surface areas, making them good adsorbents for environmental remediation [25]. Regarding this, it has been found that heavy metals from aqueous systems, including Cr(VI), Pb(II), and Mn(II) [19, 26–27].

As per the reported work, barely any studies have been reported in the extraction of nanocellulose from the defoliated plant leaves (residual/waste plant biomass) for its application as a sorption agent in heavy metal removal from aqueous systems.

Therefore, the present work deals with the synthesis of nanocellulose from defoliated leaves of the Tropical Almond (Terminalia catappa) plant and its use in eliminating a harmful heavy metal i.e., Cr(VI) from the aqueous system, which in turn promotes the circular bio-economy [28-29].

Experimental

1) Materials

Defoliated tropical Almond (Terminalia catappa) plant leaves were collected locally from the institute campus (Odisha, India) as a source of raw cellulose material for nanocellulose preparation. The collected plant leaves were properly cleaned with tap water, sun-dried and finely ground into powder using a blender. The resulting powder biomass was used for preparing nanocellulose through a chemical method. The chemicals used in this study i.e., All the chemicals are of analytical grade.

2) Preparation of nanocellulose

In order to prepare the nanocellulose, the biomass was subjected to two stages of chemical treatment, the first stage involved the treatment with dilute NaOH solution and the second stage involved the treatment with dilute H_2SO_4 solution. The NaOH treatment breaks down the biomass structure to remove lignin and hemicelluloses from the biomass [30] and the process is called delignification or pulping, whereas the H_2SO_4 treatment breaks down the complex cellulosic structures into nanoscale cellulose particles [19]. The acid helps to hydrolyze or break down the hemicelluloses and amorphous regions of cellulose. Sulfuric acid is known for its effectiveness in breaking down complex polysaccharide structures, making it a suitable choice for the hydrolysis of lignocellulosic biomass [19]. In the first stage of chemical treatment (pulping), 10 g of the powdered Tropical Almond (Terminalia catappa) leaves was taken in a beaker to which 2 wt% of NaOH was added, with a solid-to-liquid ratio of 1 by mass. The resulting mixture was mixed at a temperature of 80 °C for 2 h followed by filtration. The residue of the filtration was repeatedly washed with distilled water till neutralization and then dried. The dried pulped mass was further treated (hydrolyzed) with 20% H_2SO_4, with a solid-to-liquid ratio of 1 by mass by stirring in a magnetic stirrer in a similar condition to that of NaOH treatment for pulping of biomass. The resulting liquid suspension part was

subjected to centrifugation and the obtained solid centrifuged mass was repeatedly treated with distilled water followed by repeated centrifugation until the supernatant liquid became neutral. The resulting neutralized and centrifuged solid mass was air-dried to produce nanocellulose.

3) Characterization

3.1) FTIR analysis

The Tropical Almond (Terminalia catappa) leaves are a lignocellulosic biomass known to be made up of cellulose, hemicelluloses and lignin. Through FTIR, the chemical structure and the functional groups present in each sample were identified [26]. Such analysis can also provide information regarding structural changes that has been taken place during the formation of nanocellulose from the pristine biomass [9].

The FTIR analysis of the resulting nanocellulose was carried out through a Thermo Scientific Nicolet iS5 FTIR Spectrometer in a wave number range from 4000 cm^{-1} to 500cm^{-1}. To confirm the removal of lignin and hemicelluloses during the preparation of nanocellulose, the FTIR spectra of the nanocellulose and NaOH-treated biomass sample are compared with that of the pristine biomass sample (powdered Terminalia catappa leaves) [9].

3.2) SEM Analysis

The surface morphologies of the biomass sample, NaOH-treated sample and nanocellulose sample were studied by using a scanning electron microscope (SEM) (Zeiss, EVO 18). The SEM micrographs help to determine the change in surface microstructure of the biomass sample due to nanocellulose formation. Such kind of information may assist in describing the surface adsorption behaviour of the produced nanocellulose [31].

3.3) XRD Analysis

X-ray diffraction pattern of prepared nanocellulose was recorded through an X-ray diffractometer (Bruker AXS D8 Advance), having X-ray source Co-Kα radiation source (λ = 1.79 Å) scanned with 2θ angle ranging from 10° to 80°, operated at a voltage of 20 kV. The X-ray diffraction pattern provides information regarding the crystallinity of the produced nano-cellulose [31].

4) Removal of Cr(VI) by nanocellulose

For adsorption study or removal of Cr(VI) by nanocellulose, 10 ml of standard Cr(VI) solution, Potassium dichromate ($K_2Cr_2O_7$) was taken in a 100 ml beaker to which 10 mg nanocellulose was added and the resulting mixture was stirred at room temperature for various time-periods with the help of magnetic stirrer. At different time-period intervals, nanocellulose-treated dichromate solution was analyzed for Cr(VI) concentration through standard gravimetric analysis using lead nitrate as a precipitating agent. For carrying out adsorption isotherm studies four different concentrations (100, 200, 400, 600 mg L^{-1}) of Potassium dichromate ($K_2Cr_2O_7$) solutions were used as a source for Cr(VI).

To estimate the amount of Cr(VI) removed (mg mg^{-1}) from the aqueous solution the following equation was used:

$$q_e = \frac{C_i - C_e}{m} V \qquad \text{(Eq. 1)}$$

Where, C_i and C_e are the initial and equilibrium concentrations (mg L^{-1}), m is the mass of nanocellulose (mg) and V is the volume of the solution (L) [24–25].

The percent adsorption (%) is calculated using the equation

$$\% \text{ adsorption} = \frac{C_i - C_e}{C_i} \text{ x } 100 \qquad \text{(Eq. 2)}$$

Results and discussion

1) Fourier transform infrared spectroscopy (FTIR) analysis

Figure 1 represents the FTIR spectra of the untreated biomass (a), NaOH-treated biomass (b) and the produced nanocellulose (c) respectively. For the three constituents of lignocellulosic biomass (cellulose, hemicellulose and lignin), hydroxyl stretching vibrations are found between 3000 cm^{-1} and 3500 cm^{-1}. Such a peak is found to be more intense in NaOH-treated biomass than that of the original biomass sample and nanocellulose sample. The more intense peak in the NaOH-treated sample may be attributed to the hydrolysis factor in the said sample [27]. The lowest peak intensity of such peak in nanocellulose sample may be due to the removal of lignin suggesting a structural change as a result of formation of nano-cellulose formation. Peak around 1700–1730 cm^{-1}, corresponds to aromatic groups in lignin. The peak at 1500–1600 cm^{-1} is attributed to the C=C stretching vibration of the aromatic ring in lignin. A peak around 1450 cm^{-1} represents an aromatic skeletal ring of lignin and such a peak is absent in synthesized nanocellulose suggesting removal of lignin due to formation of nanocellulose. Peak ranging from 1170–1082 cm^{-1} corresponds to the C–O–C group of pyranose ring skeletal in cellulose. The peak in the range of 1047-900 cm^{-1} corresponds to deformation

vibrations of C-O bands in the primary alcohol of lignin. The lignin peaks are sharper and more apparent in the original biomass sample compared to the alkali-treated sample and nanocellulose. In the same context, moreover, some lignin peaks visible in the original biomass sample are absent in nanocellulose, suggesting lignin removal due to hydrolysis of the pretreated biomass sample to produce nanocellulose. On the other hand, the peak at around 899 cm^{-1} is associated with the C–O stretching and C–H vibrations of hemicelluloses [19, 27–28].

2) Scanning electron microscope (SEM) study

Figure 2 (a-f) shows the surface morphologies of the untreated biomass samples (powdered Terminalia catappa leaves), NaOH-treated biomass and produced nanocellulose sample at two different magnifications. A continuous uniform surface morphology is observed in the case of untreated biomass (Figure 2a) showing cellulose structure is covered by an amorphous phase of lignin and hemicellulose. At higher magnification for the untreated biomass (Figure 2b) the morphology of biomass shows cavity-type morphology with clearly visible boundaries. After alkali (NaOH) treatment, the original surface morphology of the biomass sample is completely changed to fibrous morphology (Figure 2c) suggesting the removal of lignin that covers the cellulose microfibrils [19] and such features are more clearly visible in the higher magnification (Figure 2d). The SEM micrograph of the produced nanocellulose sample shows a quite heterogeneous and rough morphology consisting of pores and particles of variable shapes such as elliptical, spherical, and irregular type, present independently as well as in clusters, with average particle diameter lies in the nanoscale range [32] (Figures-2e and 2f). Complete structural changes take place in the case of nanocellulose from that of the original biomass sample as well as from the NaOH-treated biomass sample biomass sample observed in higher magnified morphology (Figure 2f).

3) X-ray diffraction (XRD)study

Figure 3 shows the XRD pattern of the resulting nanocellulose. The peaks at 16.70, 34.60 correspond to the characteristic peaks of cellulose [33]. Cellulose has amorphous and crystalline parts, where the amorphous part is more vulnerable to the acid hydrolysis process for which the concentration of acid during hydrolysis has a significant effect on the crystallinity characteristics of the resulting nanocellulose. However, higher acid concentration can have an impact on both breaking the amorphous region as well as destroying the crystalline region of the produced nanocellulose [1].

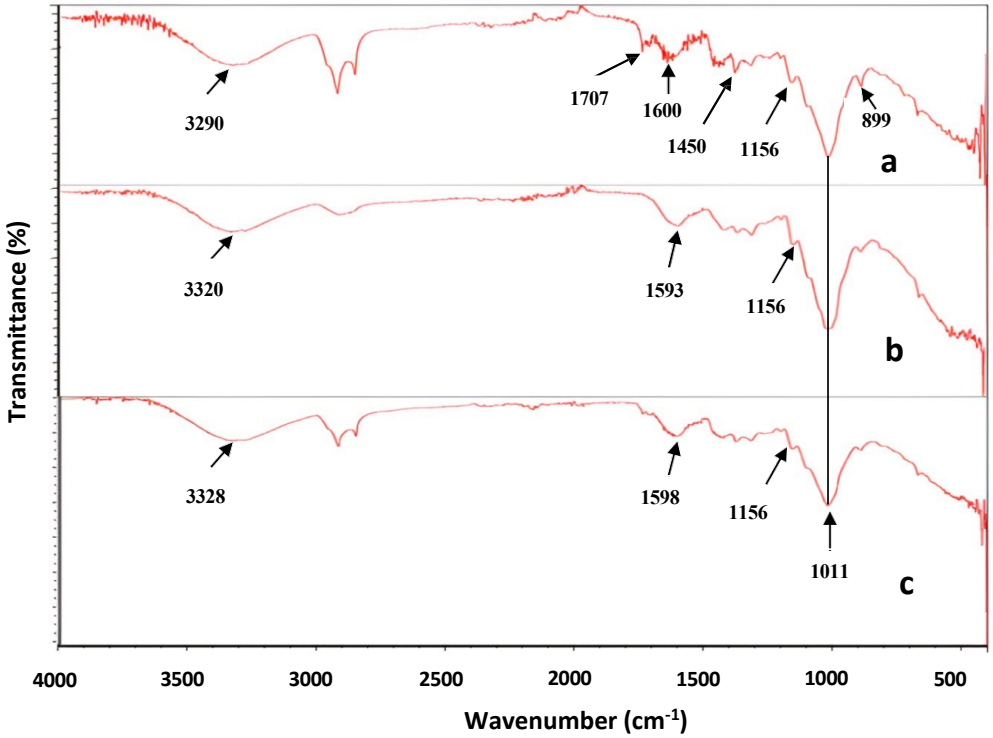

Figure 1 FTIR spectra of (a) untreated biomass, (b) NaOH treated biomass, (c) resulting nanocellulose.

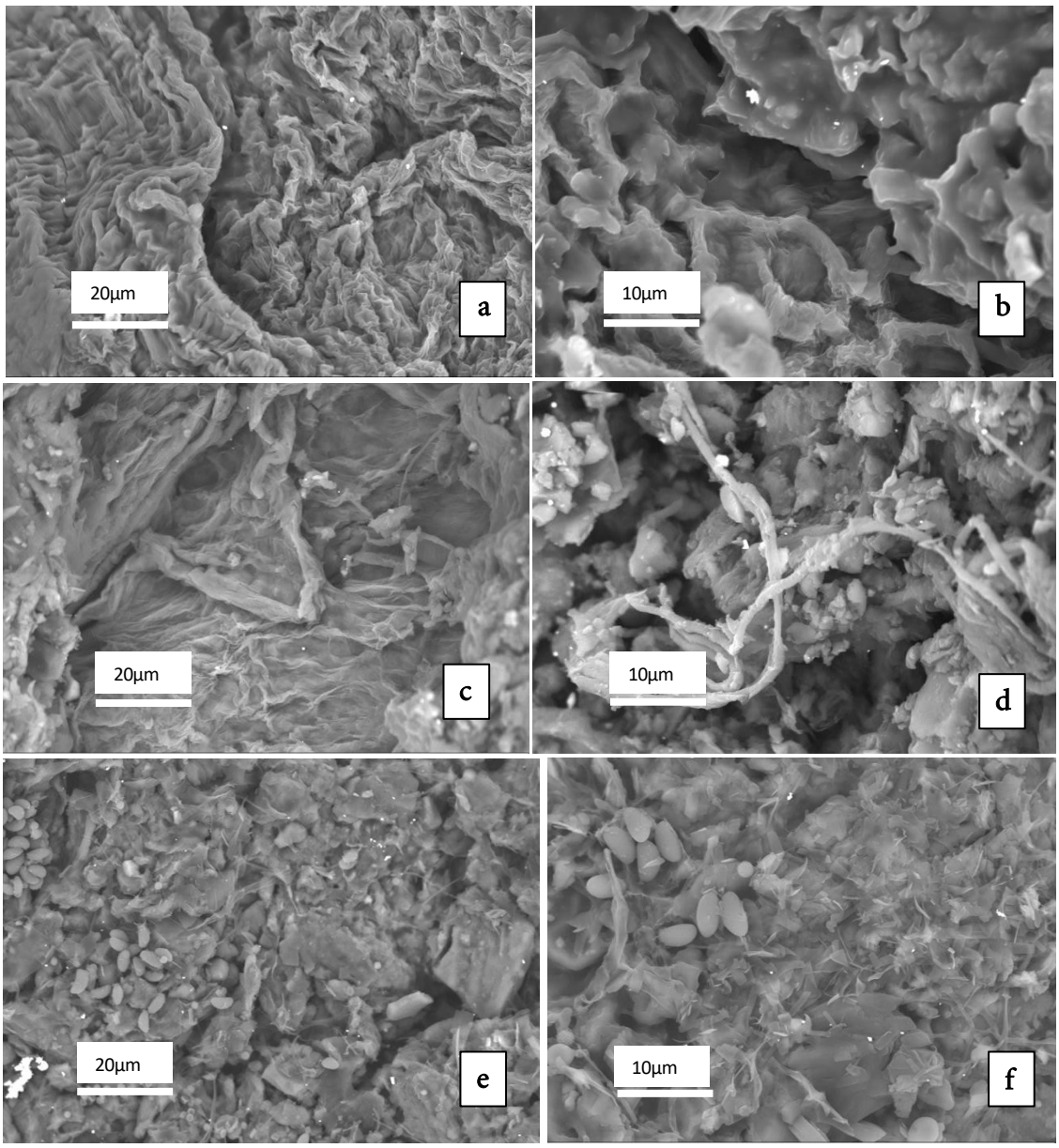

Figure 2 SEM micrograph at two different magnifications: (a&b) untreated biomass, (c&d) NaOH-treated biomass, and (e&f) resulting nanocellulose.

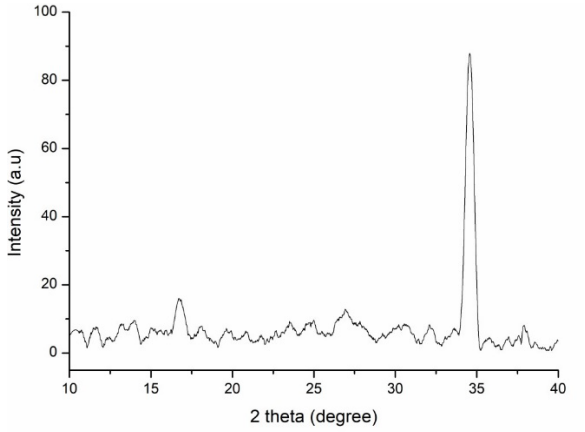

Figure 3 XRD pattern of the produced nanocellulose.

For nanocellulose, the high-intensity peak at 34.6° describes the crystalline character of the substance, and the intensity value illustrates the degree of crystalline structure. The crystallinity index was calculated through the integration method by using Eq 3.

$$\text{Crystallinity} = \frac{A_{Cryst}}{A_{Total}} \text{ x } 100 \qquad \text{(Eq. 3)}$$

Where, Acrys area under the crystalline peaks and Atotal is the area under all the peaks. The crystallinity index of the produced nanocellulose is found to be 42.08%. The value is quite lower than the reported one [1], which may be due to the varying concentration of H_2SO_4 during hydrolysis. The decreased value of crystallinity of nanocellulose will facilitate more hydroxyl groups exposed to improve the availability and accessibility of cellulose, to enhance the overall novel properties of nanocellulose [33].

4) Chromium (VI) removal by nanocellulose

The efficacy of the produced nanocellulose in terms of Cr(VI) removal from aqueous medium has been studied concerning the time period of treatment and through adsorption isotherm and kinetic studies.

4.1) Effect of the time period of treatment of nanocellulose on Cr(VI) removal

Figure 4 shows the effect of the time period of treatment/contact of nanocellulose on Cr(VI) removal. It has been found that at room temperature (36°C) with an increase in the time period, there is a gradual increase in chromium removal and a maximum Cr(VI) removal of 98.4% is achieved for a treatment period of 75 min. The increase in Cr(VI) removal with an increase in time is due to the greater interaction between the nanocellulose adsorbent and Cr(VI) ions [34]. Upon further increase in time period to 90 min there is no significant change in chromium removal observed, suggesting almost complete adsorption of the metal ions, i.e. equilibrium is achieved due to the non-availability of active sites on the nanocellulose surface [34–35].

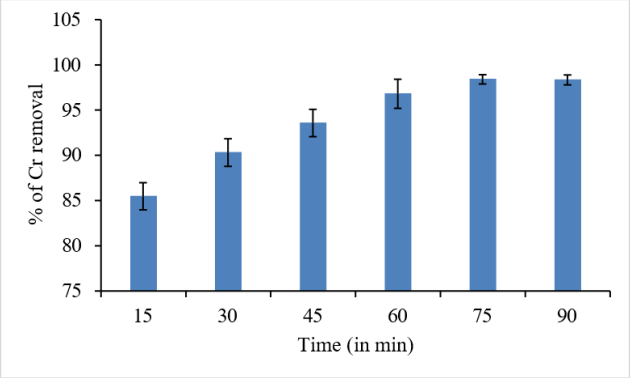

Figure 4 Effect of the time period of treatment of nanocellulose on Cr(VI) removal.

4.2) Adsorption isotherm

The adsorption isotherm represents the relationship between the amount of adsorbate adsorbed by a unit weight of adsorbent and the amount of solute remaining in the solution at equilibrium and such kind of study shows the particular adsorbent suitability in the application of water pollution control [35]. In this regard, Langmuir and Freundlich isotherm studies were found to be suitable for describing short-term and mono-component adsorption of metal ions by different adsorbents [36].

Freundlich model

The Freundlich isotherm in linear form is given as follows:

$$\ln q = \ln K + 1/n \ln C_e \quad \text{(Eq. 4)}$$

where C_e is the equilibrium concentration of adsorbate in the solution and q is the amount of adsorbate adsorbed per unit mass of adsorbent (nanocellulose), K and 1/n are constants, representing adsorption capacity and adsorption intensity or surface heterogeneity respectively [34, 37]. A plot of q vs. produces a straight line with a slope = 1/n and intercept = ln K. When $0 < 1/n < 1$, the adsorption is favourable, and when $1/n > 1$, the adsorption is unfavourable [37].

According to this isotherm, the adsorption of metal ions takes place on heterogeneous surfaces with multilayer adsorption and the adsorption increases with an increase in concentration [37].

Langmuir adsorption isotherm

Langmuir adsorption isotherm suggests that the adsorption takes place with monolayer adsorption on specific homogeneous surfaces containing a finite number of adsorption sites. The linear form of this isotherm is given as

$$\frac{C_e}{q} = \frac{1}{qmax\ k} + \frac{C_e}{qmax} \quad \text{(Eq. 5)}$$

Where C_e (mg L^{-1}) is the equilibrium concentration of adsorbate, q_e (mg g^{-1}) is the amount of adsorbate adsorbed per unit mass of adsorbent, q_{max}(mg g^{-1}) is the maximum adsorption capacity, k (L mg^{-1}) is Langmuir constant related to the energy of adsorption [34, 37]. A plot of $\frac{C_e}{q}$ vs. $Ce$is a straight line with slope $\frac{1}{q\ max}$ and intercept $\frac{1}{qmax\ k}$ [37] and from the slope, q_{max} can be calculated.

Table 1 represents the adsorption parameters of Freundlich and Langmuir for Cr(VI) removal by producing nanocellulose adsorbent. The 1/n value 0.865 for the present adsorption study in Freundlich adsorption isotherm suggests that the nanocellulose adsorbent for Cr(VI) removal is effective due to its greater affinity for this metal ion [34–35, 37].

The 'k' value of Langmuir adsorption isotherms indicates the interaction between adsorbate and the surface. If the value of 'k' is relatively greater it indicates that there is a strong interaction between the adsorbate and adsorbent [34] and hence greater removal of the solute from the aqueous system. In the present case, the 'k' value is found to be 0.833(L mg^{-1}). Also from this study, the maximum adsorption

capacity, q_{max} is found to be 0.222 mg mg^{-1}. Upon comparison to the R^2 value, as provided in Table 1, it can be said that the present adsorption process preferentially follows the Freundlich adsorption, involving multilayer heterogeneous adsorption of Cr(VI) on nanocellulose [38].

Table 1 Adsorption isotherm parameters of Cr(VI) removal by produced nanocellulose

Isotherm	Adsorption parameters	Cr(VI)
Freundlich	1/n	0.865
	K (mg g^{-1})	1.882
	R^2	0.999
Langmuir	qmax (mg mg^{-1})	0.222
	k (L mg^{-1})	0.833
	R^2	0.992

4.3) Adsorption kinetics

The kinetic behaviour of the Cr(VI) removal using nanocellulose was determined with the pseudo-first and pseudo-second-order kinetic model. The pseudo-first-order kinetic model and pseudo-second-order kinetic model equations are presented in Equations (6) and (7), respectively [39].

The first-order kinetic equation can be expressed as:

$$ln(q_e - q_t) = ln\, q_e - k_1 t \quad \text{(Eq. 6)}$$

The second-order kinetic equation can be expressed as:

$$\frac{t}{q_t} = \frac{1}{k_2 q_e^2} + \frac{t}{q_e} \quad \text{(Eq. 7)}$$

Where, q_t and q_e are the adsorption capacity (g/g) at a particular time period 't' and equilibrium respectively, k_1 (L min^{-1}) and k_2 (mg mg^{-1} min^{-1}) is the pseudo-first-order and pseudo-second-order adsorption-rate constant [40].

Based on the findings presented in Table 2, the correlation coefficient (R^2) value suggests that the adsorption kinetic data were more fitted with the pseudo-2nd-order model than the pseudo-1st-order model [41]. This indicates that the pseudo 2nd order model is better suited for explaining the adsorption mechanism of Cr(VI) ions onto the surface of the prepared nanocellulose. These results also imply that the Cr(VI) sorption on the nanocellulose surface is through chemisorption. Moreover, prior studies on Cr(VI) adsorption have also demonstrated the superiority of the pseudo 2nd order model over other kinetic models for describing the Cr(VI) removal mechanism [41].

Table 2 Adsorption kinetics parameters of Cr(VI) removal by produced nanocellulose

Kinetics model	Parameters	Values
Pseudo first order	Q_e	35.67
	K_1	-0.0236
	R^2	0.9162
Pseudo second order	Q_e	35.67
	K_2	0.030
	R^2	0.9933

4.4) Adsorption mechanism

After chromium adsorption, the XRD pattern of nanocellulose is shown in Figure 5, which shows attenuation and reduction in the peak intensities of all the characteristic peaks of the nanocellulose before adsorption (Figure 3). Such kind of observation may be attributed to the binding of chromium ions on the nanocellulose surface, which results in alteration of the XRD pattern after Cr(VI) adsorption [42].

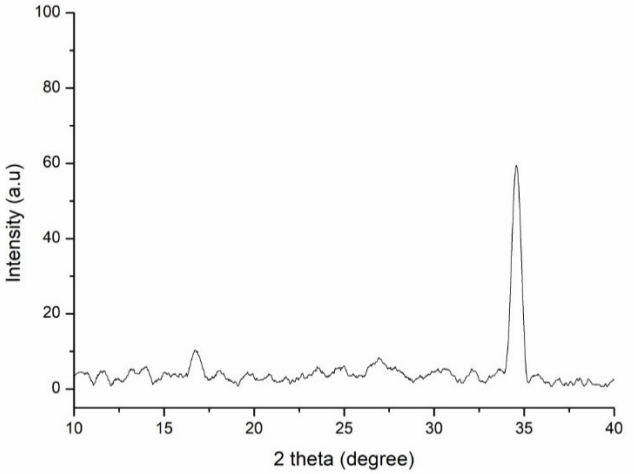

Figure 5 XRD pattern of the produced nanocellulose after adsorption.

The sorption behaviour of nanocellulose for Cr(VI) can be described due to the presence of ultrafine pores, high surface area, and heterogeneous morphology along with phenomena like ion exchange and chemical complexation. The ion exchange mechanism involves the adsorption of hazardous metal ions by replacing other ions (K^+, Na^+, H^+) already associated with the nanocellulose surface. The chemical complexation involves the interactions of various groups such as the carboxyl ($-COO^-$) and hydroxyl (-OH) groups of the nanocellulose with the particular hazardous metal ions. For this reason, increasing surface area, ultrafine pores, surface heterogeneity and surface function-

alization are necessary for greater adsorption of hazardous metal ions [38, 43–44].

From the studies like FTIR, SEM and XRD, the probable mechanism of Cr(VI) adsorption on nanocellulose surface can be explained as follows:

(i) The presence of a functional hydroxyl group (Figure 1(c)) in nanocellulose can adsorb Cr(VI) ions by electrostatic means. The hydroxyl groups are negatively charged and exhibit electrostatic attraction toward cationic wastewater pollutants.

(ii) The presence of ultra-fine pore, nano-size particles resulting in high surface area, along with rough surface morphology as evidenced from SEM micrographs (Figure 2 (e&f)) corresponds to the greater adsorption capacity of Cr(VI) on the produced nanocellulose.

(iii) The peak intensities difference in XRD patterns of the produced nanocellulose before and after adsorption suggests Cr(VI) adsorption through the combined effects of presence of –OH functional groups as well as by surface adsorption due to the availability of ultra-fine pores, nanoparticles and surface roughness.

Conclusion

The study reveals the successful preparation of nanocellulose from defoliated Tropical almond (Terminalia catappa) leaves highlights for its application in Cr(VI) removal from water stream. The study also reveals a substantial structural and morphological change happened in the biomass sample due to nanocellulose preparation. With a crystallinity degree of 42% determined by XRD, the resulting nanocellulose emerges as an effective adsorbing agent, demonstrating a remarkable ~98% Cr(VI) removal from aqueous streams. The adsorption of Cr(VI) is assisted by the electrostatic interaction between the –OH groups of the nanocellulose as well as due to the high adsorption capacity of porous, rough surface containing nano size materials of the produced nanocellulose. This research signifies an innovative approach to utilize abundantly available waste plant biomass for sustainable applications in heavy metal removal from the water stream, alternatively encouraging the concept of a circular bioeconomy.

Conflict of interest

On behalf of all authors, the corresponding author states that there is no conflict of interest.

References

[1] Wulandari, W.T., Rochliadi, A., Arcana, I.M. Nanocellulose prepared by acid hydrolysis of isolated cellulose from sugarcane bagasse, in: IOP Conf Ser Mater Sci Eng, Institute of Physics Publishing, 2016.

[2] Salas, C., Nypelo, T., Rodriguez-Abreu, C., Carrillo, C., Rojas, O.J. Nanocellulose properties and applications in colloids and interfaces, Current Opinion in Colloid & Interface Science, 2014, 19, 383–396.

[3] Li, W., Yue, J., Liu, S. Preparation of nanocrystalline cellulose via ultrasound and its reinforcement capability for poly(vinyl alcohol) composites, Ultrasonics Sonochemistry, 2012, 19, 479–485.

[4] Trache, D., Tarchoun, A.F., Derradji, M., Hamidon, T.S., Masruchin, N., Brosse, N., Hussin, M.H. Nanocellulose: From fundamentals to advanced applications. Frontiers in Chemistry, 2020, 8, 392.

[5] Owonubi, S.J., Agwuncha, S.C., Malima, N.M., Shombe, G.B., Makhatha, E.M., Revaprasadu, N. Non-woody biomass as sources of nanocellulose particles: A Review of Extraction Procedures. Frontiers in Energy Research, 2021, 9.

[6] Barbash, V., Yaschenko, O. Preparation, properties and use of nanocellulose from non-wood plant materials, [Online] Available from: https://www.intechopen.com/chapters/73744

[7] Phanthong, P. , Reubroycharoen, P., Hao, X., Xu, G., Abudula, A., Guan, G. Nanocellulose: extraction and application, Carbon Resources Conversion, 2018, 1(1), 32–43.

[8] Ng, H.M., Sin, L.T., Tee, T.T., Bee, S.T., Hui, D., Low, C.Y., Rahmat, A.R., Extraction of cellulose nanocrystals from plant sources for application as reinforcing agent in polymers, Composites Part B: Engineering, 2015, 75, 176–200.

[9] Song, K., Zhu, X., Zhu, W., Li, X. Preparation and characterization of cellulose nanocrystal extracted from Calotropis procera biomass, Bioresource and Bioprocessing, 2019, 6(1), 45.

[10] Gupta, G.K., Shukla, P. Lignocellulosic biomass for the synthesis of nanocellulose and its eco-friendly advanced applications, Frontier in Chemistry, 2020, 8, 601256.

[11] Yu, X., Jiang, Y., Wu, Q., Wei, Z., Lin, X., Chen, Y. Preparation and characterization of cellulose nanocrystal extraction from Pennisetum hydridum fertilized by municipal sewage sludge via sulfuric acid hydrolysis, Frontiers in Energy Research, 2021, 9, 774783.

[12] Rizal, S., Yahya, E.B., Abdul Khalil, H.P.S., Abdullah, C.K., Marwan, M., Ikramullah, I., Muksin, U. Preparation and characterization of nanocellulose/chitosan aerogel scaffolds using chemical-free approach, Gels, 2021, 7(4), 246.

[13] Kusmono,R.F., Listyanda, M.W., Wildan, M.N. Ilman, Preparation and characterization of cellulose nanocrystal extracted from ramie fibers by sulfuric acid hydrolysis, Heliyon, 2020, 6(11), e05486.

[14] Rasri, W., Thu, V.T., Corpuz, A., Nguyen, L.T. Preparation and characterization of cellulose nanocrystals from corncob via ionic liquid [Bmim][HSO_4] hydrolysis: effects of major process conditions on dimensions of the product, RSC Advances, 2023, 13, 19020–19029.

[15] Pramanick, B. Preparation and characterization of nanocellulose fibre incorporated poly methyl methacrylic acid based superabsorbent gel. Materials Today: Proceedings, 2022, 60, 1994-2000.

[16] Nicole, L., Rosario, G., Diego, B.M., de O.V. Gabriela, M., Pablo, C., Fernanda, G. Ma., Josй, V.B., Hugo, C., Mary, L. Preparation and characterization of a novel nanocellulose-derivative as a potential radiopharmaceutical agent, Waste and Biomass Valorization, 2022, 13, 173–183.

[17] Raju, V., Revathiswaran, R., Subramanian, K. S., Parthiban, K. T., Chandrakumar, K., Anoop, E.V., Chirayil, C.J. Isolation and characterization of nanocellulose from selected hardwoods, viz., Eucalyptus tereticornis Sm. and Casuarina equisetifolia L., by steam explosion method. Scientific Reports, 2023, 13(1), 1199.

[18] Mahardika, M., Abral, H., Kasim, A., Arief, S., Asrofi, M. Production of nanocellulose from pineapple leaf fibers via high-shear homogenization and ultrasonication, Fibers, 2018, 6, 28.

[19] Mehanny, S., Abu-El Magd, E.E., Ibrahim, M., Farag, M., Gil-San-Millan, R., Navarro, J., El Habbak, A.E.H., El-Kashif, E. Extraction and characterization of nanocellulose from three types of palm residues, Journal of Materials Research and Technology, 2021, 10, 526–537.

[20] Velбzquez, M.E., Ferreiro, O.B., Menezes, D.B., Corrales-Ureca, Y., Vega-Baudrit, J.R., Rivaldi, J.D. Nanocellulose extracted from Paraguayan residual agro-industrial biomass: Extraction process, physicochemical and morphological characterization, Sustainability (Switzerland), 2022, 14(18), 11386.

[21] Ramos, M., Valdйs, A., Garrigys, M. C. Multifunctional applications of nanocellulose-based nanocomposites. In: Multifunctional polymeric nanocomposites based on cellulosic reinforcements, 2016, William Andrew Publishing.

[22] Yang, R., Aubrecht, K.B., Ma, H., Wang, R., Grubbs, R.B., Hsiao, B.S., Chu, B. Thiol-modified cellulose nanofibrous composite membranes for chromium (VI) and lead (II) adsorption, Polymer, 2014, 55(5), 1167–1176.

[23] Muthulakshmi, L., Rajini, N., Nellaiah, H., Kathiresan, T., Jawaid, M., Rajulu, A.V. Preparation and properties of cellulose nanocomposite films with in situ generated copper nanoparticles using Terminalia catappa leaf extract, International Journal of Biological Macromolecules, 2017,95, 1064–1071.

[24] Zhu, H., Jia, S., Wan, T., Jia, Y., Yang, H., Li, J., Yan, L., Zhong, C. Biosynthesis of spherical Fe_3O_4/bacterial cellulose nanocomposites as adsorbents for heavy metal ions, Carbohydrate Polymers, 2011, 86(4), 1558–1564.

[25] Guerra, F.D., Attia, M.F., Whitehead, D.C., Alexis, F. Nanotechnology for environmental remediation: Materials and applications, Molecules, 2018, 23(7), 1760.

[26] Singh, K., Arora, J.K., Sinha, T.J.M., S. Srivastava, S. Functionalization of nanocrystalline cellulose for decontamination of Cr(III) and Cr(VI) from aqueous system: Computational modeling approach, Clean Technologies and Environmental Policy, 2014, 16, 1179–1191.

[27] Morбn, J.I., Alvarez, V.A., Cyras, V.P., Vбzquez, A. Extraction of cellulose and preparation of nanocellulose from sisal fibers, Cellulose, 2018, 15, 149–159.

[28] Pula, B., Ramesh, S., Pamidipati, S., Doddipatla, P. A comparative study of greener alternatives for nanocellulose production from sugarcane bagasse, Bioresources and Bioprocessing, 2021, 8, 132.

[29] Casau, M., Dias, M.F., Matias, J.C.O., Nunes, L.J.R. Residual biomass: A comprehensive review on the importance, uses and potential in a circular bioeconomy approach, Resources, 2022, 11(4), 35.

[30] Nasir, M., Hashim, R., Sulaiman, O., Asim, M. Nanocellulose: Preparation methods and applications, in: Cellulose-reinforced nanofibre composites: Production, properties and applications, Elsevier Inc., 2017, pp. 261–276.

[31] Emam, A.A., Abo, S.A., Faraha, F.H., Kamal, A.M. Gamal, M. Basseem, M. Modification and characterization of nano cellulose crystalline from Eichhornia crassipes using citric acid: An ad-sorption study, Carbohydrate Polymers, 2020, 240, 116202.

[32] Jeevanandam, J., Barhoum, A., Chan, Y.S., Dufresne, A., Danquah, M.K., Review on nanoparticles and nanostructured materials:

History, sources, toxicity and regulations, Beilstein Journal of Nanotechnology, 2018, 9, 1050–1074.

[33] Zhang, S., Zhang, F., Jin, L., Liu, B., Mao, Y., Liu, Y., Huang, J. Preparation of spherical nanocellulose from waste paper by aqueous NaOH/thiourea, Cellulose, 2019, 26, 5177–5185.

[34] Ali, A., Saeed, K., Mabood, F. Removal of chromium (VI) from aqueous medium using chemically modified banana peels as efficient low-cost adsorbent, Alexandria Engineering Journal, 2016, 55, 2933–2942.

[35] Mahardiani, L., Ilfama, R., Saputro, S., Pranolo, S.H., Septianing, P.W. Nanocellulose obtained from biomass as advance adsorbent for methylene blue and crystal violet, Journal of Physics: Conference Series, 2021, 012015.

[36] Al-Sou'od, K. Adsorption isotherm studies of chromium (VI) from aqueous solutions using Jordanian pottery materials, APCBEE Procedia, 2012, 1, 116–125.

[37] Kalam, S., Abu-Khamsin, S.A., Kamal, M.S., Patil, S. Surfactant adsorption isotherms: A review, ACS Omega, 2021, 6, 32342–32348.

[38] Alzahrani, F.M., Amari, A., Katubi, K.M., Alsaiari, N.S., Tahoon, M.A. The synthesis of nanocellulose-based nanocomposites for the effective removal of hexavalent chromium ions from aqueous solution, Open Chemistry, 2022, 20, 970–983.

[39] Mohamed, S.H., Hossain, M.S., Kassim, M.H.M., Balakrishnan, V., Habila, M.A., Zulkharnain, A., Zulkifli, M., Yahaya, A.N.A. Biosorption of Cr(VI) using cellulose nanocrystals isolated from the waterless pulping of waste cotton cloths with su-percritical CO_2: Isothermal, kinetics, and thermodynamics studies, Polymers (Basel), 2022, 14(5), 887.

[40] Alsaiari, N.S., Katubi, K.M., Alzahrani, F.M., Amari, A., Osman, H., Ben Rebah, F., Tahoon, M.A. Synthesis, characterization and application of polypyrrole functionalized nanocellulose for the removal of cr(Vi) from aqueous solution, Polymers, 2021, 13(21), 3691.

[41] Mahmoud, A.E.D., Fawzy, M., Hosny, G., Obaid, A. Equilibrium, kinetic, and diffusion models of chromium(VI) removal using Phragmites australis and Ziziphus spina-christi biomass, International Journal of Environmental Science and Technology, 2021, 18, 2125–2136.

[42] Mzinyane, N.N., Mnqiwu, K.M., Moukangoe, K.M. Adsorption of hexavalent chromium Ions using pine sawdust cellulose fibres, Applied Sciences (Switzerland), 2023, 13(17), 9798.

[43] Dim, P.E., Mustapha, L.S., Termtanun, M., Okafor, J.O. Adsorption of chromium (VI) and iron (III) ions onto acid-modified kaolinite: Isotherm, kinetics and thermodynamics studies, Arabian Journal of Chemistry, 2021, 14(4), 103064.

[44] Salama, A., Abouzeid, R., Leong, W.S., Jeevanandam, J., Samyn, P., Dufresne, A., Bechelany, M., Barhoum, A. Nanocellulose-based materials for water treatment: Adsorption photocatalytic degradation, disinfection, antifouling, and nanofiltration, Nanomaterials, 2021, 11(11), 3008.